

Magnetic Enhancement in Cobalt-Manganese Alloy Clusters

Shuangye Yin, Ramiro Moro, Xiaoshan Xu, and Walter A. de Heer

School of Physics, Georgia Institute of Technology, Atlanta, Georgia 30332, USA

(Received 10 October 2006; published 15 March 2007)

Magnetic moments of Co_NMn_M and Co_NV_M clusters ($N \leq 60$; $M \leq N/3$) are measured in molecular beams using the Stern-Gerlach deflection method. Surprisingly, the per atom average moments of Co_NMn_M clusters are found to increase with Mn concentration, in contrast to bulk CoMn. The enhancement with Mn doping is found to be independent of cluster size and composition in the size range studied. Meanwhile, Co_NV_M clusters show reduction of average moments with increasing V doping, consistent with what is expected in bulk CoV. The results are discussed within the virtual bound states model.

DOI: [10.1103/PhysRevLett.98.113401](https://doi.org/10.1103/PhysRevLett.98.113401)

PACS numbers: 36.40.Cg, 75.20.Hr, 75.50.Ee, 82.80.Rt

Magnetism of clusters has been intensively investigated in the past decade. Significant enhancements of magnetism are often observed due to the low coordination numbers and slight lattice expansion. Experiments on Fe, Co, and Ni clusters show that they are ferromagnetic and have enhanced magnetic moments when they contain less than about 1000 atoms [1]. Rh is found to be ferromagnetic in clusters with magnetic moments of as large as 0.8 Bohr magnetons (μ_B) per atom, even though bulk Rh is paramagnetic [2]. Mn clusters were determined to be ferromagnetic or ferrimagnetic in the size range of 5–99, while bulk Mn is antiferromagnetic [3,4]. These discoveries together with theoretical work on cluster magnetism have enriched the understanding of nanomagnetism. While early work mainly concentrated on elemental clusters, there are some studies of alloy species in the search for novel nanomagnetic materials. Stern-Gerlach (SG) experiments have been performed on BiCo [5], DyTe, and DyBi clusters [6]. Recently, our own work on BiMn [7] has shown highly magnetic cluster species as well as ferromagnetic and antiferromagnetic coupling behavior in these clusters. Magnetic enhancement is also found in chemically synthesized CoRh nanoparticles [8]. For magnetic alloys, the most important property is the saturation magnetization, which is usually presented as a function of average electron number in the Slater-Pauling plot. The major trends were first explained by Slater and Pauling, based on a rigid band model [9,10]. But the generally accepted explanation is from Friedel [11], who considered the formation of virtual bond states (VBS) near impurity atoms in the host. To our knowledge, there has been no attempt to study the Slater-Pauling behavior in magnetic alloy clusters. It is interesting to examine if the physical picture developed from bulk alloys is still valid in alloy clusters.

The study of deposited alloy magnetism in nanoparticles is both an experimental and theoretical challenge. It is difficult to control the stoichiometry in nanoparticles using chemical methods. The nanoparticles inevitably interact with each other and with the substrate, which makes the measurements difficult and explanations ambiguous. These

difficulties are resolved in molecular cluster beams [12] since the clusters, once formed, are isolated from contaminations and other interactions during the measurement. Moreover, their chemical composition is accurately determined using high-resolution mass spectrometry methods. Here, we present magnetic measurements on Co_NMn_M and Co_NV_M clusters, for $N \leq 60$ and $M \leq N/3$. The photoionization thresholds as well as reactivities were studied in molecular beams [13,14], but their magnetic properties have not been reported. The experimental method used here is described elsewhere [15,16]. Briefly, alloy clusters are produced in a cryogenically cooled pulsed laser vaporization source, which is maintained at low temperature using a temperature controlled closed cycle cryogenic refrigerator. A high power laser pulse (Continuum Surelite I20, 355 nm) is focused on a 2 mm diameter alloy target rod. Several alloy rods are used in these experiments: $\text{Co}_{0.85}\text{Mn}_{0.15}$ and $\text{Co}_{0.5}\text{Mn}_{0.5}$ rods were purchased from Alfa Aesar; $\text{Co}_{0.88}\text{V}_{0.12}$ rods were produced using a home-made induction-heating furnace. A pulse of helium is injected in the source to form the cold cluster beam, which is collimated to a width of 0.3 mm before entering the inhomogeneous field of a Stern-Gerlach magnet that causes the magnetic clusters to deflect. The deflection (d) of a cluster is proportional to the average magnetization (M_{eff}) in the magnetic field, determined by

$$d = KM_{\text{eff}}(dB/dz)/mv^2 \quad (1)$$

where K is the geometry factor of the apparatus, m and v are the mass and speed of the cluster, dB/dz is the magnetic field gradient.

M_{eff} is related to the intrinsic magnetic moment of the cluster (μ) [17,18]. Both for clusters in molecular beams and for supported clusters, the magnetization is in the same direction of the magnetic field. When $\mu B/k_B T \ll 1$, $M_{\text{eff}} \approx \mu^2 B/3k_B T$ and when $\mu B/k_B T \gg 1$, $M_{\text{eff}} \approx \mu$; but there are differences for intermediate fields [18]. At the experimental conditions for the results presented in this Letter, M_{eff} can be approximately expressed using the Langevin equation,

$$M_{\text{eff}} = \mu[\coth(\mu B/k_B T) - k_B T/\mu B]. \quad (2)$$

Hence, the intrinsic value of the magnetic moment is determined from the deflections. The deflected clusters are photoionized using an ArF excimer laser (Lambda Physik Optex, 193 nm), and detected in a position-sensitive time-of-flight mass spectrometer (PSTOFMS) [19], which simultaneously measures the cluster deflections and their masses (Fig. 1). The method requires that mass resolution be traded for position sensitivity so that it is restricted to small clusters (i.e., less than 100 atoms), to preserve adequate mass resolution. The composition of the alloy clusters species is determined from their masses, which in most cases is unambiguous. Statistics are used for the few cases where ambiguity exists.

The magnetic moments (μ) of Co_NMn_M clusters are determined using Eqs. (1) and (2) (Fig. 2). The total moments generally increase with the addition of Co or Mn atoms. The size effect of Mn doped Co clusters is remarkable. In Fig. 3(a), we fix the total of atoms ($N_t = N + M$) and plot at the average moment per atom ($\langle\mu\rangle = \mu/N_t$) as a function of impurity concentration ($x = M/N_t$), for several representative cluster sizes.

The slopes of these curves are equivalent to the change of total moment after substituting one Co atom by one Mn atom. For Co_NMn_M clusters, the average moments increase with increasing Mn concentration. The average magnetic moment enhancement after substitution of a Co with a Mn atom is $1.7\mu_B$, for all the alloy clusters in our experiments. The average moment also depends on the

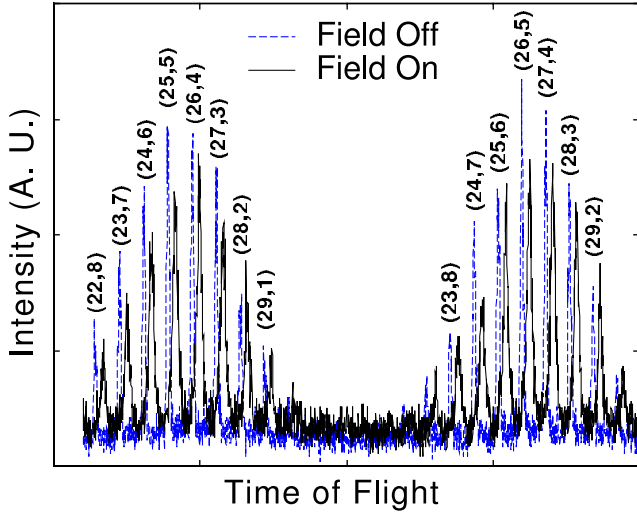


FIG. 1 (color online). Part of the position-sensitive mass spectrum of Co_NMn_M clusters. Dashed line is the spectrum without magnetic field. Solid line is with magnetic field (0.98 T). Magnetic deflections cause the cluster mass peaks to shift to the right when the magnet is activated. The magnetization is determined from the deflections of the mass peaks. The compositions of the Co_NMn_M clusters as determined from the masses are denoted as (N, M) .

cluster size, as discussed below. In separate experiments using Mn rich samples, it is seen that the increasing trend only persists for Mn concentrations up to 30% to 40%, after which the average moment decreases with increasing Mn concentration.

This magnetic enhancement is contrasted with that of bulk CoMn, where the substitution of Co with Mn atoms tends to decrease the average moment [20] by about $6.0\mu_B$ per substitution. The observed trends in bulk are explained by the formation of virtual bond states (VBS) near the impurity state. For ferromagnetic transition metals, it is well known that the magnetic moment is due to the d electrons, which occupy spin-up and spin-down bands that are split by the exchange interaction:

$$n_d = n_d^\uparrow + n_d^\downarrow,$$

where n_d , n_d^\uparrow , and n_d^\downarrow are the total, majority, and minority d band occupations, respectively. The average magnetic moments (in units of μ_B) are determined from the imbalance between spin-up and spin-down occupations, $\mu = n_d^\uparrow - n_d^\downarrow$, which can be written as

$$\mu = 2n_d^\uparrow - n_d. \quad (3)$$

If the spin-up bands are fully occupied, the material is called a strong magnet; otherwise, it is a weak magnet [21]. For a strong magnet, $n_d^\uparrow = 5$ so that $\mu = 10 - n_d$. While this explains the right-hand-side slope of the Slater-Pauling curve, it is not applicable for early transition metal impurities in Co or Ni, which manifest themselves as the fast dropping branches that deviate from the Slater-Pauling curve. In this case (as for the bulk [11,21,22]), one has to consider the formation of VBS near the impurity sites. If the difference between the atomic number of the impurity

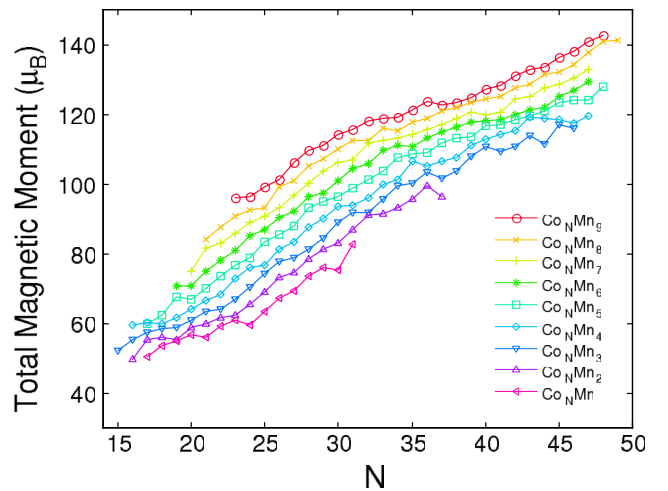


FIG. 2 (color online). Total magnetic moment of Co_NMn_M clusters as a function of N . Each series represents clusters with the same number of Mn atoms N . The experimental uncertainty is about $1.5\mu_B$.

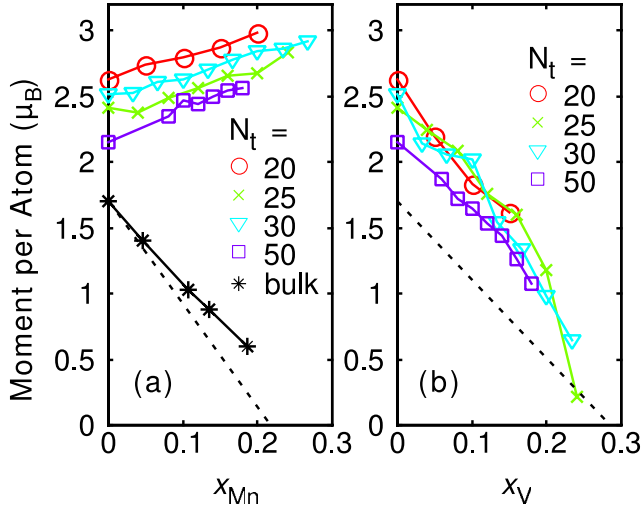


FIG. 3 (color online). Magnetic moments per atom of Co_NMn_M (a) and Co_NMn_M (b) clusters. Representative cluster sizes ($N + M$) are shown; other clusters have similar behavior. The data for bulk CoMn are from [20]. Dotted line is the expected magnetic moments assuming the VBS are above the Fermi level.

and the host $\Delta Z = Z_{\text{impurity}} - Z_{\text{host}}$ is sufficiently large ($-\Delta Z > 2$), the VBS will rise above E_F because electrons are less attracted to the impurity ions. As a result, the VBS may be completely unoccupied. Note that the degeneracy of the VBS is exactly 5 for each impurity atom as first pointed out by Friedel [11] (See also Refs. [21,22]). In this case, we have $n_d^{\uparrow} = 5 - 5x$ and $n_d = n_d^{\text{Host}} + \Delta Zx$, where x is the impurity concentration per atom. From Eq. (3), we find the average moment of the alloy to be

$$\mu = 10 - n_d^{\text{Host}} - (\Delta Z + 10)x = \mu^{\text{Host}} - (\Delta Z + 10)x. \quad (4)$$

Since $\Delta Z + 10$ is always positive, this explains the decreasing trend of the magnetic moment of transition metal ferromagnets with increased doping with early transition metals like V and Mn.

For Mn impurities in a Co host, $\Delta Z = -2$. The slope of average moment as a function of x from Eq. (4) is expected to be $-8\mu_B$. The trend of CoMn bulk ($-6\mu_B$ slope) is close to this expectation. The difference can be explained by the fact that $\Delta Z = -2$ is not large enough to cause the VBS to rise entirely above E_F . From band structure calculations of dilute Mn impurities in a Co host [23], the Mn local moments are found to have both antiferromagnetic and ferromagnetic couplings with the Co, where the antiferromagnetic state has the lower energy. In both cases, the calculated average moment decreases with increasing Mn concentration.

However, in CoMn clusters, we observe a positive slope, suggesting that the VBS are below E_F . In this case, $n_d^{\uparrow} = 5$ and $n_d = n_d^{\text{Host}} + \Delta Zx$. From Eq. (3), we find the average

moment of the alloy to be

$$\mu = 10 - n_d^{\text{Host}} - \Delta Zx = \mu^{\text{Host}} - \Delta Zx. \quad (5)$$

With $\Delta Z = -2$ for Mn impurity in Co host, one finds the slope to be $2\mu_B$, which is close to the $1.7\mu_B$ found in Fig. 3(a). Since the spin-up bands in Co_NMn_M clusters are filled, they should follow the Slater-Pauling curve. This suggests an avenue for synthesizing high moment materials based on clusters.

Experiments on Co_NV_M clusters are more consistent with the case that the VBS are above E_F . The average magnetic moments as a function of V concentration are plotted in Fig. 3(b). For Co_NV_M clusters, the average moments generally decrease with increasing V concentration. The decreasing trends are similar for all clusters with only a few exceptions (Co_{41}V_2 , Co_{17}V_2 , Co_{23}V_3 , Co_{25}V_4 , and Co_{19}V_6 , which are not shown in the figure). Although CoV alloy magnetism data are not available for comparison, calculations show [23] that V in Co is the perfect case to form VBS well above the Fermi level because of the large nuclear charge difference $\Delta Z = -4$. Experimental data for Fe-V, Ni-V, and CoNi-V alloys [21,22] all agree with this picture. According to Eq. (4), the predicted slope is $-6\mu_B$, consistent with our experimental measurements [Fig. 3(b)]. Note that this effect cannot be explained by considering the Co moment only. If V atoms were considered as inert additions to Co clusters, the slope would have been $-2\mu_B$.

Another observation is that the magnetic enhancement by doping with Mn atoms is uniform and does not depend

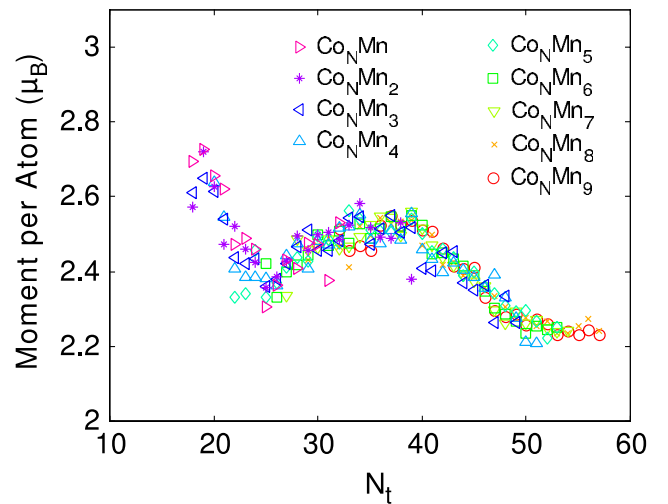


FIG. 4 (color online). Normalized average moment for Co_NMn_M clusters. The contribution due to the electron deficiency of Mn compared to Co (i.e., 1.7 electrons per substituted atom) is subtracted. The normalized average moments only depend on the total number of atoms, which indicates the presence of the VBS below E_F . If the spin-up band of the VBS is completely below E_F , then the strong magnetism picture applies and the enhancement is $2\mu_B$. We observe that the enhancement is $1.7\mu_B$, which is reasonably close to this prediction.

dent on the size or composition of the Co_NMn_M clusters. This is illustrated in Fig. 4 where we subtracted the enhancement by the Mn atoms (i.e., we subtracted $1.7\mu_B$ for each Mn atom), which results in a universal curve. Hence, we treat the Mn atoms as if they were Co atoms, however with an electron deficiency of 1.7 per atom. The resulting curve is consistent with pure Co clusters. This implies that, except the valence difference, Mn atoms play the same role as Co atoms. Note that the ionic radii of Mn and Co (in 12 coordinated metals) are very close (1.26 and 1.25 Å, respectively) [24]. Further note that in bulk, up to 20% Mn can be dissolved in solid Co without altering the host crystal structure [25]. These facts suggest that substitution of Co atoms with Mn atoms in clusters does not significantly alter the geometric structure of the clusters. Besides forming the additional VBS above E_F , the band structure of the cluster appears to be essentially unchanged.

In summary, a magnetic moment enhancement is found for cobalt clusters doped with manganese atoms, which is opposite to that of the bulk. In contrast, doping vanadium atoms in cobalt clusters reduces the average magnetic moment, which is consistent with bulk behavior. The magnetic enhancement does not depend on the cluster size and composition, indicating the robustness of the geometric and electronic structure upon doping with Mn. Hence, the magnetic moments of these alloy clusters can still be approximately understood in an electronic band picture similar to bulk alloys. This emphasizes the intrinsic connections between the electronic properties of clusters and the bulk. We interpret the overall trends of experimental results (linear dependence on impurity concentration, and size-dependence on total number of atoms) using a virtual bound states model that was initially developed for bulk alloys. The prediction from the model qualitatively agrees with experiments for CoV clusters. However, in order to explain the magnetic enhancement trends for CoMn clusters, the assumption that VBS are below Fermi level has to be made, the mechanism of which is not clear in this framework. Theoretical investigations using more advanced tools, such as density functional theory, will definitely shed light on this point. Such studies will also help to elucidate more details about the local moment distribution, size-dependence, and detailed electronic structures in these alloy clusters, as has been demonstrated in earlier studies [26].

This work is supported by NSF and DARPA. The authors are grateful to Uzi Landman for stimulating

discussions.

-
- [1] I. M. L. Billas, A. Chatelain, and W. A. de Heer, *Science* **265**, 1682 (1994).
 - [2] A. J. Cox, J. G. Louderback, and L. A. Bloomfield, *Phys. Rev. Lett.* **71**, 923 (1993).
 - [3] M. B. Knickelbein, *Phys. Rev. Lett.* **86**, 5255 (2001).
 - [4] M. B. Knickelbein, *Phys. Rev. B* **70**, 014424 (2004).
 - [5] T. Hihara, S. Pokrant, and J. A. Becker, *Chem. Phys. Lett.* **294**, 357 (1998).
 - [6] S. Pokrant, C. Herwig, T. Hihara, and J. A. Becker, *Eur. Phys. J. D* **9**, 509 (1999).
 - [7] S. Y. Yin, X. S. Xu, R. Moro, and W. A. de Heer, *Phys. Rev. B* **72**, 174410 (2005).
 - [8] D. Zitoun, M. Respaud, M. C. Fromen, M. J. Casanove, P. Lecante, C. Amiens, and B. Chaudret, *Phys. Rev. Lett.* **89**, 037203 (2002).
 - [9] J. C. Slater, *J. Appl. Phys.* **8**, 385 (1937).
 - [10] L. Pauling, *Phys. Rev.* **54**, 899 (1938).
 - [11] J. Friedel, *Nuovo Cimento Suppl.* **7**, 287 (1958).
 - [12] W. A. de Heer, *Rev. Mod. Phys.* **65**, 611 (1993).
 - [13] S. Nonose, Y. Sone, and K. Kaya, *Z. Phys. D* **19**, 357 (1991).
 - [14] G. M. Koretsky, K. P. Kerns, G. C. Nieman, M. B. Knickelbein, and S. J. Riley, *J. Phys. Chem. A* **103**, 1997 (1999).
 - [15] R. Moro, X. S. Xu, S. Y. Yin, and W. A. de Heer, *Science* **300**, 1265 (2003).
 - [16] R. Moro, S. Y. Yin, X. S. Xu, and W. A. de Heer, *Phys. Rev. Lett.* **93**, 086803 (2004).
 - [17] S. N. Khanna and S. Linderoth, *Phys. Rev. Lett.* **67**, 742 (1991).
 - [18] X. S. Xu, S. Y. Yin, R. Moro, and W. A. de Heer, *Phys. Rev. Lett.* **95**, 237209 (2005).
 - [19] W. A. De Heer and P. Milani, *Rev. Sci. Instrum.* **62**, 670 (1991).
 - [20] J. Crangle, *Philos. Mag.* **2**, 659 (1957).
 - [21] A. R. Williams, V. L. Moruzzi, A. P. Malozemo, and K. Terakura, *IEEE Trans. Magn.* **19**, 1983 (1983).
 - [22] A. P. Malozemoff, A. R. Williams, and V. L. Moruzzi, *Phys. Rev. B* **29**, 1620 (1984).
 - [23] V. S. Stepanyuk, R. Zeller, P. H. Dederichs, and I. Mertig, *Phys. Rev. B* **49**, 5157 (1994).
 - [24] C. Kittel, *Introduction to Solid State Physics* (Wiley, New York, 1996).
 - [25] K. Ishida and T. Nishizawa, in *Binary Alloy Phase Diagrams*, edited by T. B. Massalski (ASM International, Materials Park, OH, 1990).
 - [26] R. Fournier and D. R. Salahub, *Surf. Sci.* **238**, 330 (1990).